Journal of Controlled Release 341 (2022) 329–340

Contents lists available at ScienceDirect

Journal of Controlled Release

journal homepage: www.elsevier.com/locate/jconrel

Traceless antibiotic-crosslinked micelles for rapid clearance of intracellular bacteria

Xingyue Yang [a,b], Qian Qiu [a,b], Gengqi Liu [a,b], He Ren [a,b], Xiaojie Wang [a,b], Jonathan F. Lovell [c], Yumiao Zhang [a,b,*]

[a] School of Chemical Engineering and Technology, Tianjin University, 300350, PR China
[b] Key Laboratory of Systems Bioengineering (Ministry of Education) Tianjin University, Tianjin 300072, PR China
[c] Department of Biomedical Engineering, The State University of New York at Buffalo, Buffalo, NY 14260, USA

ARTICLE INFO

Keywords:
Intracellular bacteria
Hydrophobic modification
Self-immolation
Drug-crosslinked micelles
Toxicity

ABSTRACT

Effective delivery of antimicrobial agents to intracellular pathogens represents a major bottleneck for a wide variety of infectious diseases. To address this, we developed SIR-micelles(+), as a new delivery vehicle comprising antibiotic-loaded micelles with rapid self-immolation within cells for targeted delivery to macrophages, where most intracellular bacterial reside. After phagocytosis, SIR-micelles(+) rapidly release the pristine antibiotic after the cleavage of the disulfide bonds by intracellular reducing agents such as glutathione (GSH). Colistin, a hydrophilic and potent "last-resort" antibiotic used for the treatment of drug-resistant bacterial infection, was encapsulated in SIR-micelles with 40% yield and good short-term storage stability. Hydrophobic moieties and mannose ligands in SIR-micelles(+) enhanced the delivery of colistin into macrophages. The traceless and thiol-responsive release of colistin effectively eliminated intracellular *Escherichia coli* within twenty minutes. In a murine pneumonia model, SIR-micelles(+) significantly reduced bacterial lung burden of multidrug-resistant *Klebsiella pneumoniae*. Furthermore, SIR-micelles(+) improved the survival rate and reduced the bacterial burden of organs infected by intracellular bacteria transferred from donor mice. Using this formulation approach, the nephrotoxicity and neurotoxicity induced by antibiotic were reduced by about 5– 15 fold. Thus, SIR-micelles(+) represent a new class of material that can be used for targeting treatment of intracellular and drug-resistant pathogens.

1. Introduction

Recurrent and chronic infections caused by intracellular bacteria have been a long-standing lethal burden on human public health [1]. Generally, most of the bacteria could be eliminated by the phagocytosis and digested in lysosomes, however intracellular bacteria such as *Mycobacterium, Listeria, Shigella, Brucella, Methicillin-resistant Staphylococcus aureus and Klebsiella pneumoniae* are able to escape from lysosomes. They can reside and proliferate in cytoplasm or intracellular vacuoles to evade immune attack, eventually leading to cell apoptosis [2–4]. *K. pneumoniae* is considered as one of the most dangerous gram-negative pathogens causing infections including pneumonia, urinary tract infections and lower biliary tract infections, leading to higher mortality in neonates and elderly people with impaired immunity [5]. Usually, *klebsiella pneumoniae* has traditionally been considered an extracellular bacteria. However, mounting evidence shows that several strains invade and survive intracellularly after being taken up into macrophages, persisting in klebsiella-containing vacuoles and causing serious infections [6,7].

Macrophages, are the main host for intracellular pathogens and thus are also used as the target for intracellular pathogen treatments. In order to deliver antibiotics to macrophages, delivery systems should meet the following requirements simultaneously: (1) maintain physiological stability and structural integrity when circulating in blood without significant degradation; (2) actively target and enter macrophages by efficient phagocytosis or endocytosis; (3) release antibiotics in a responsive and timely manner to escape endosomes or lysosomes. (4) be safe without inducing significant toxicity. However, the current therapeutic paradigms still face many challenges and usually solving one of them might also conflict with another [8]. Liposomes, chitosan/fucoidan and poly

* Corresponding author at: School of Chemical Engineering and Technology, Tianjin University, 300350, PR China; Key Laboratory of Systems Bioengineering (Ministry of Education) Tianjin University, Tianjin 300072, PR China.
E-mail address: ymzhang88@tju.edu.cn (Y. Zhang).

https://doi.org/10.1016/j.jconrel.2021.11.037
Received 31 August 2021; Received in revised form 6 November 2021; Accepted 22 November 2021
Available online 26 November 2021

(lactic-*co*-glycolic acid) (PLGA) have been developed to deliver antibiotics for bacteria treatment, although effective encapsulation of hydrophilic antibiotics in nanoparticles with high drug loading is challenging [9–11]. One approach is hydrophobic modification of existing antibiotics but releasing active form of antibiotics in a timely and precisely-controlled manner is difficult [12]. Mannose ligands have been conjugated with delivery systems for the active targeting delivery owing to the receptors (CD206) on the surface of macrophages [13]. Empty cell envelopes with complete lipopolysaccharide structures have also been used to load ciprofloxacin for targeted treatment of intracellular bacteria [14]. The metals of silver and gold exhibited a synergistic antibacterial effect in nanoparticles, but potential long-term toxicity induced by inorganic metals may raise safety concerns [15,16]. Other strategies include the use of mesoporous silica modified with lipid bilayer for responsive release of gentamicin for intracellular *staphylococcus aureus* infection [17]. Despite these promising approaches, few delivery vehicles can integrate all the aforementioned desirable features with respect to intracellular delivery of antibiotics.

Multidrug resistance and toxicity induced by antibiotics are two central issues for the development of antimicrobials [18,19]. Intracellular bacterial infections are usually associated with the emergence of drug-resistance where suboptimal antibiotics are used for intracellular infection treatment. To control the spread of the multidrug resistant (MDR) bacteria globally, especially for those intracellular MDR-bacteria [20], there is a need to develop new antibiotics or alternatively new antimicrobial formulations using established antibiotics. Colistin had been used as the "last resort" for clinical MDR bacterial infection management once bacteria have developed resistance mechanisms to almost all other antibiotics [21]. However, the severe side effects of nephrotoxicity [22,23] and neurotoxicity [24] induced by colistin are the bottleneck for its wide use in clinics. We previously reported antibiotic-crosslinked micelles, termed ABC-micelles to reduce the nephrotoxicity and neurotoxicity of colistin, however only loaded colistin could be released and crosslinked drug as carriers were unable to responsively release cargo in a self-immolation manner [25]. For the targeting intracellular bacteria, this prior work did not address macrophage targeting or cell penetration moieties. Rifampicin was known to be one of the most effective antibiotics for intracellular infection treatment [26], but it is not recommended to be used alone due to high risk of resistance [27]. Serious hepatotoxicity induced by rifampicin is also a concern so it was often used in combination with fusidic acid that can penetrates well in granulocytes for treating intracellular antimicrobials [28,29]. Taken together, there is a need to deliberately develop effective and safe drug delivery systems that can reconcile all these challenges for the treatment of intracellular multidrug-resistant bacterial infection.

In the present work, we design a nanoplatform of antibiotic-crosslinked micelles with a rapid self-immolation rate, termed SIR-micelles(+), for the treatment of intracellular infections including multidrug-resistant *klebsiella pneumoniae* (Table S1). Pluronic F127 (F127) was activated by grafting a hydrophobic and self-immolative linker so that hydrophilic amine-containing colistin was able to cross-link with modified F127, thus forming SIR-micelles *via* one-pot synthesis method, followed by removal of free surfactant by ultracentrifugation at low temperature [30–33]. The primary amine groups in colistin, responsible for the severe nephrotoxicity and nephrotoxicity, can be masked by SIR-micelles that maintain stable and safe when circulating in blood. The hydrophobic moiety deliberately designed in the linker could facilitate the phagocytosis of SIR-micelles similarly as proteins or peptides attached with hydrophobic tails that can penetrate and transport easily into cells [34–36]. Also, with the targeting ligand mannose attached to SIR-micelles, SIR-micelles(+) were formed that can actively deliver colistin in macrophages. Once phagocytized in macrophages, SIR-micelles(+) rapidly release the pristine colistin to effectively kill intracellular multidrug resistant bacteria in responsive to higher concentration of intracellular glutathione [37]. The dual functions of the linker including hydrophobic modification and self-immolation are key for the intracellular delivery of antibiotics and traceless and rapid release in cells.

2. Experimental section/methods

2.1. Material and reagents

Pluronic F127(Sigma, America); 2,9,16,23-tetra-tert-butyl-29,31H-phthalocyanine (BPc, Sigma, America) *P*-nitrophenyl chloroformate, NPC (HEOWNS, China); Glutathione, GSH (HEOWNS, China); Colistin sulfate (YuanyeBio-Technology, Shanghai, China); 4-aminophenyl-alpha-D-mannopyranoside (Jiuding Chemical); Dithiodiacetic acid (Energy Chemical, Shanghai, China); Dithiothreitol (Energy Chemical, Shanghai, China); Dimethylaminopyridine (YuanyeBio-Technology, Shanghai, China); Triethylamine (Kermel, China); Tryptone (OXOID); Beef extract (OXOID); Agar powder (Aladdin, Beijing, China); DMEM (Gibco, America); FBS (Yeasen biotech, Shanghai, China); Penicillin-Streptomycin Liquid (Solarbio, Beijing, China); APC F4/80 antibody (123,115, Biolegend, America); FITC (Solarbio, Beijing, China). benzene (HEOWNS, China); DMSO (Kermel, China); All Enzyme Linked Immunosorbent Assay Kit (Elisa) kits were purchased from Solarbio. Other materials and solvents were purchased from Aladdin unless noted otherwise. The RFP-expressing *E. coli* MG 1655 was kindly provided by Professor Kun Zhao and *K. pneumoniae* Y. 8401 was obtained from Prof. Pengfei Wang's group at Shanghai Jiao Tong University.

2.2. Synthesis of F127-SH

0.1 mmol F127 was dissolved in 20 mL of dichloromethane, and 0.8 mmol dimercaptodiacetic acid, 0.8 mmol of 1-(3-dimethylaminopropyl)-3-ethylcarbodiimide hydrochloride (EDC), 0.8 mmol 4-dimethylaminopyridine (DMAP) were sequentially added to the F127 solution to react overnight under stirring at room temperature. The product obtained by precipitation with cold diethyl ether was dialyzed with 6000–8000 MWCO dialysis bag. Next, 1.6 mmol of dithiothreitol (DTT) and 220 μL of triethylamine (TEA) were dropwise added into the purified dialysate mentioned above. After reaction overnight under Argon atmosphere, the final product of F127-SH was obtained by freeze drying after dialysis filtration (MWCO = 6000–8000).

2.3. Synthesis of SIR-F127 and SIS-F127

The synthesis and characterization of SIS-linker and SIR-linker were conducted according to previously reported methods [38]. SIR-linker (0.05 mmol) or SIS-linker (0.05 mmol) was added into F127-SH (0.02 mmol) respectively for reaction in 20 mL of dichloromethane overnight. The solution was subjected to rotary evaporation and vacuum drying at 35 °C. Subsequently, the collected powder was dissolved in 20 mL of DD water and then was centrifuged (3000 *g*, 25 °C) for 30 min. The supernatant was freeze-dried under vacuum to obtain purified powder of SIS-F127 or —SIR-F127. NPC-F127 was also prepared as below. Briefly, 1.005 g of *p*-nitrophenyl chloroformate (NPC) and 10 g of dehydrated Pluronic F127 were dissolved in 35 mL of anhydrous benzene with stirring for 24 h at 25 °C under Argon atmosphere, then the product of NPC-F127 was collected after rotary evaporation and precipitation in cold diethyl ether.

2.4. Characterization of SIR-F127 and SIS-F127

First, the contact angle of blended mixture of SIR-F127 and pristine F127 (5%, *w/v*, total concentration) were measured by Contact Angle Meter. Next, different percent of SIR-F127 (0, 20%, 40%, 60%, 80%, 100%) in the mixture of SIR-F127 and pristine F127 were prepared. Then, 10 mg 2,9,16,23-tetra-tert-butyl-29,31H-phthalocyanine (BPc, Sigma) was dissolved in 1 mL dichloromethane, and 25 μL of such BPc stock solution above was dropwise added into 250 μL of 5% (wt) of SIR-

F127 and pristine F127 aqueous mixture. After stirring for 3 h, 25 μL of BPc encapsulated blended micelles was added into 24-well plate containing 1×10^6 macrophages (J774A.1). Cells were incubated for 4 h at 37 °C with 5% CO_2 and were washed twice with PBS. Then the mean fluorescent intensity (MFI) of the cells were detected at excitation/emission of 610/700 nm 2 h after cell lysis by the addition of phosphate buffer solution with 1% Triton-X. The uptake of SIS-F127 micelles into macrophages was also measured similarly as SIR-F127 by replacing SIR-F127 by SIS-F127.

2.5. Preparation and characterization of SIR-micelles

To prepare SI-micelles including SIR-micelles and SIS-micelles, 5 mg colistin was dissolved in 50 μL of 0.1 M sodium bicarbonate aqueous solution and then it was added dropwise into 500 μL of SIR-F127 (5%, *w/v*) in pH 9 buffer solution with addition of 0.5 M NaCl under stirring. After stirring for 3 h at room temperature, the un-crosslinked and loosely-bound micelles were washed away by centrifugal ultrafiltration (Millipore) with a MWCO of 100 KD for three times, 0.5 M fresh NaCl solution was added back to start new washes. NPC-micelles and SIS-micelles were synthesized similarly as SIR-micelles described above. To prepare SIR-micelles(+), 1 mg of 4-aminophenyl-alpha-D-mannopyranoside (Jiuding Chemical) was added with stirring for 2 h to react with SIR—F127. The yield of colistin loaded in SIR-micelles was measured using 2,4,6-Trinitrobenzenesulfonic acid (TNBSA) method and corresponding calculation process as follows: yield of colistin (%) = (colistin loaded into *main-ABCs*) / (initial addition excluding colistin as crosslinker) × 100. The size and zeta potential of micelles were measured by dynamic light scattering (DLS, Malvern) and transmission electron microscopy (TEM) with negatively staining by 1% uranyl acetate. The colistin release rate in Fig. 2i was measured under reductive condition when subjected to dialysis of 10 mM GSH in PBS at 37 °C.

2.6. In vitro internalization by macrophage

Macrophages J774A.1 were seeded in 96-well plate in concentration of 1×10^5 cells per well followed by incubation at 37 °C for 24 h. FITC-labeled colistin formulations including free colistin, NPC-micelles, SIS-micelles, SIR-micelles, SIR-micelles(+) were co-cultured with the cells for 4 h at 37 °C with 5% CO_2. The mean fluorescent intensity (MFI) was assessed by microplate reader (Tecan Infinite 200® Pro) at excitation/emission 495 nm/525 nm 2 h after the cells were lysed with 1% Triton-X100 in PBS.

To further detect the uptake of different colistin formations into macrophages, J774A.1 cells were plated in 6-well plates at a density of 1×10^6 per well. Cells were cultured overnight and then were washed twice with PBS. Next, drug formations labeled with FITC (1 μg/mL) were incubated with cells for 4 h before being digested with pancreatin. The cells were incubated with 2.5 μg/mL of APC-F4/80 antibody for 1 h on ice, which were used to specifically label macrophages, and then were analyzed by flow cytometry.

Besides, macrophages J774A.1 were seed in 35 mm glass-bottom Petri dish at a density of 5×10^5 per dish and incubated overnight. After co-culturing with different colistin formations labeled with FITC (1 μg/mL) for 4 h, the cells were incubated with lysotracker for 30 min for labeling lysosome and then were fixed with formaldehyde (4%) for 10 min before stained with Hoechst for 10 min. The cells were resuspended in PBS for the analysis by laser scanning confocal microscopy.

2.7. In vitro antimicrobial effect on extracellular and intracellular bacteria

Minimum inhibitory concentrations (MICs) of free colistin, SIS-micelles and SIR-micelles against *MDR-KP* with or with no addition of GSH were assessed using checkerboard dilution method. J774A.1 macrophages were seeded in 96-well plates at a density of 1×10^5 per well in DMEM medium with 10 (wt)% heat-inactivated fetal bovine serum (FBS) and incubated for 24 h. The cells were washed with DMEM at least twice and then were infected with carbapenem-resistance *K. pneumoniae* Y. 8401(*CR-KP*) for 1 h at a multiplicity of infection (MOI) of 100 to 1. The cells were rinsed three times with PBS and were co-cultured with 100 μg/mL of gentamycin for 30 min to kill extracellular bacteria. After being rinsed with PBS three times to remove the gentamycin, the cells were treated with PBS and various colistin formations at a concentration of 64 μg/mL for 12 h. The cells were lysed with 200 μL of 0.1% Triton-X and then the lysates were diluted in a series of PBS containing 0.1% Triton-X were plated on LB agar medium to determine the CFUs of intracellular bacteria.

RFP-*E. coli* MG1655 that could survive intracellularly also were tracked at different timepoints with fluorescent microscope. Briefly, macrophages J774A.1 were plated in 35 mm glass-bottom *peri* dish at a density of 1×10^6 per dish and incubated for 24 h. The infection process and the treatment of gentamycin were the same as described above. Then the cells were co-cultured with free drug, SIS-micelles, SIR-micelles and SIR-micelles(+) at concentration of 64 μg/mL and the images of intracellular bacteria were recorded at different time points using fluorescent microscopy.

2.8. In vivo toxicity of free drug and SIR-micelles(+)

8-week-old female CD-1 mice were obtained from Charles River Beijing Co., Ltd. (Beijing, China). For nephrotoxicity and hepatotoxicity, mice were intravenously injected with free drug (1, 3, 5 mg/mL), SIR-micelles (5, 10, 15 mg/mL) *via* tail vein every day for 7 consecutive days ($n = 4$ per group). Serum was collected to be used for the analysis of nephrotoxicity by measuring neutrophils gelatinase-associated lipid delivery proteins (NGAL) and blood urea nitrogen (BUN). Hepatotoxicity was evaluated by measuring alkaline phosphatase (AKP). Urine was collected for the evaluation of nephrotoxicity by measuring kidney injury molecule 1 (KIM-1). In addition, mice were sacrificed after the last injection and kidney tissues were collected for histopathology analysis. For neurotoxicity evaluations of free drug and SIR-micelles, the brain tissues were homogenized and then subject to centrifugation at 1000 rcf for 10 min at 4 °C to collect supernatant. The homogenate was collected and used for the evaluation of catalase activity and caspase-3 measurements according to published protocol [25].

2.9. In vivo treatment of intracellular pneumonia infection

To evaluate the antibacterial efficacy on intracellular bacteria *in vivo*, 8-week-old mice (female, CD-1) were intranasally infected with 4×10^7 CFUs of *K. pneumoniae* Y. 8401 per mouse to establish pneumonia infection model. After 24 h, mice were administrated both intravenously (5 mg/mL) and intranasally (1 mg/kg) or only intravenously administered (5 mg/kg) of different colistin formations including free colistin, NPC-micelles, SIS-micelles, SIR-micelles, SIR-micelles(+) daily for 3 consecutive days ($n = 3$ per group). The lung tissues were rinsed with 5 mL cold sterile PBS to extract cells. The cells were incubated with PBS containing 100 μg/mL of gentamycin and 0.1% FBS at 37 °C for 30 min to kill the extracellular bacteria and then were washed with PBS at least twice to remove remaining gentamycin. The cells were resuspended in 200 μL 0.1% Triton-X and 10-fold serial dilutions were prepared in 0.1% Triton-X in PBS. The lysates were plated on LB agar medium and incubated at 37 °C for 24 h to determine the CFU values of intracellular bacteria. Meanwhile, lung tissues were collected for histological analysis.

2.10. In vivo treatment of transferred intracellular bacterial infection

To further assess the *in vivo* therapeutic effect of drugs on intracellular bacterial infection, the model bacteremia caused by intracellular bacterial transferred from another *K. pneumoniae* Y. 8401 infected mice

was established in this study. Briefly, 8-week-old female balb/c mice purchased from Charles River Beijing Co., Ltd. (Beijing, China) were infected with 5×10^7 CFUs of *CR-KP* intraperitoneally. 24 h after infection, the abdominal cavity was washed with 5 mL of sterile cold PBS in the clean room and then the peritoneal lavage fluid was centrifuged at 1000 xg at 4 °C for 10 min to collect the cell pellet. The cells were co-cultured with PBS containing 100 μg/mL of gentamycin and 0.1% FBS at 37 °C for 30 min to kill the extracellular *CR-KP* bacteria. The cells were rinsed with sterile PBS three times to remove the remaining gentamycin. The cells from three mice as donors were merged and then were injected intravenously into acceptor mouse. 2 h after infection, the acceptor mice were treated with PBS, or 5 mg/kg free colistin, NPC-micelles, SIS-micelles, SIR-micelles or SIR-micelles(+), respectively daily for 3 consecutive days ($n = 3$ per group). The survival, body weights and health conditions were recorded during the period of treatment. Then organs were collected and homogenized after the last injection. The CFUs of organs including heart, liver, spleen, lung, and kidney were determined by plating serial dilution of homogenate on LB agar medium at 37 °C for 24 h.

2.11. Pharmacokinetics and biodistribution

8-week-old female CD-1 mice were intravenously injected with 5 mg/kg of FITC-labeled free drug or SIR-micelles ($n = 3$ for each group). And the plasma was obtained at different time points by facial blood collection. Colistin in the plasma were extracted with the mixture of distilled water and acetonitrile (7:3, *v*/v) and then the supernatants were subjected to fluorescence detection at excitation/emission wavelength of 495 nm/525 nm on microplate reader. 24 h after intravenous injection of drug formations, major organs were collected to be imaged by IVIS (Night OWLII LB 983, Berthold technologies) at excitation/emission of 495 nm/525 nm. Then the organs were homogenized in the mixture of distilled water and acetonitrile (7:3, v/v) and the concentrations of FITC-labeled colistin in the supernatants were measured.

3. Results and discussion

3.1. Generation of reduction-sensitive self-immolative F127 (SIR—F127)

To enhance phagocytosis, we first synthesized two reduction-sensitive self-immolative linkers (denoted as SIR-linker with higher hydrophobicity and rapid self-immolation rate and SIS-linker with slow self-immolation rate as control). Their synthesis routes and characterization are shown in Fig. S1. The terminal hydroxyl groups of F127 were then converted to thiols (see the synthetic route in Fig. S2, NMR spectrum in Fig. S4) so that SIR-linker or SIS-linker could be grafted to F127, generating SIR-F127 and SIS-F127 (collectively referred to as SI-F127 and SIR/SIS mean self-immolation with rapid/slow reduction rates) (Fig. S3). After chemical modification, the terminal nitrophenyl carbonate of SI-F127 became reactive to colistin (as either crosslinker or as loaded drug) or mannose (4-aminophenyl-alpha-D-mannopyranoside as targeting ligand) so that self-immolative colistin-crosslinked micelles

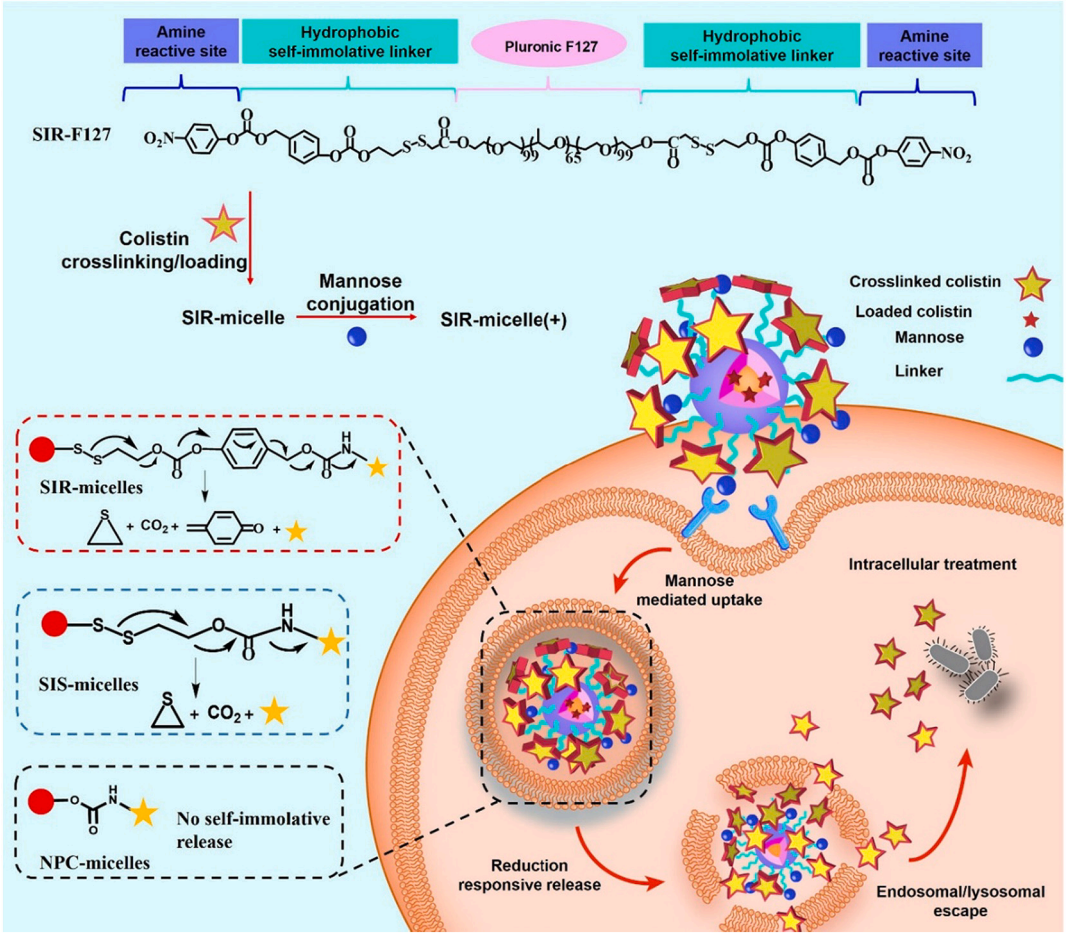

Fig. 1. Schematic illustration of the treatment of intracellular bacterial infections using SIR-micelles(+). SIS-micelles with slow self-immolation rate and NPC-micelles with no self-immolation are used as controls. SIR-F127 has three moieties: pristine F127 used for conjugation scaffold and micelle formation; hydrophobic and self-immolative moiety used for cell penetration and traceless drug release; amine active moiety used for colistin or mannose crosslinking and conjugation. SIR-micelles(+) can be easily generated by adding colistin and mannose successively in SIR-F127 aqueous solution.

with rapid/slow reduction rates (termed SIR-micelles and SIS-micelles, respectively) could be formulated *via* one-pot synthesis approach by simply adding colistin and mannose in chemically modified F127 (SI-F127) aqueous solution. As a control, non-self-immolative micelles were also prepared using *p*-nitrophenyl chloroformate (NPC) to activate F127 and the corresponding micelles are termed NPC-micelles. The SIR-micelles with the conjugation of mannose targeting ligands were denoted as SIR-micelles(+). After uptake in macrophages, the disulfide bond of SIR-micelles(+) was reduced by the intracellular GSH, rapidly releasing pristine colistin for the intracellular bacterial treatment (Fig. 1).

3.2. Generation and characterization of SIR-micelles(+)

After modification, the hydrophobicity of F127 aqueous solutions increased, revealed by the contact angle values of various 10 (wt)% of blended pristine F127, SIS-F127, and SIR-F127 solutions shown in Fig. 2a and Fig. S5–6. In order to verify enhanced phagocytosis, a fluorescent dye (2,9,16,23-tetra-tert-butyl-29,31H-phthalocyanine, BPc) was encapsulated in 10 (wt)% of blended pristine F127 and SIR-F127 solutions with a different percent of each polymer component, followed by incubation of BPc-encapsulated blended micelles with macrophages. Fluorescence was measured in cells following incubation. As shown in Fig. 2b, more fluorescence was detected in cells with the increase of SIR-F127 percent in blended solutions, indicating enhanced phagocytosis induced by SIR-F127 after conjugation of the hydrophobic linker. In contrast, SIS-F127 exhibited less phagocytosis, compared with the same concentration of SIR-F127 counterpart likely owing to the less hydrophobicity. After hydrophobic modification, SIR-F127 remains water-soluble and can form micelles. After direct addition of colistin, a part of the amine-containing colistin was crosslinked with SIR-F127 micelles, sealing the rest of colistin in SIR-F127 micelles, forming SIR-micelles with a yield of 40% (Fig. 2c). By contrast, hydrophilic colistin was unable to be encapsulated with regular F127 micelles without such trapping effect. Next, mannose ligands were conjugated by simply adding them in SIR-micelle aqueous solution, which did not significantly change the entrapment yield of SIR-micelles (38%) with a zeta potential of 10 mV because of the presence of uncross-linked positively charged colistin on the surface of micelles (Fig. 2d). Transmission electron microscopic (TEM) images of SIR-micelles(+) reveal a morphology of sphere-like shape, although some crosslinking possibly occurred between nanoparticles (Fig. 2e). Dynamic light scattering (DLS) measurement revealed the size of SIR-micelles(+) to be around 190 nm (Fig. 2f), which is larger than colistin NPC-micelles, as shown in Fig. S7. The nanoparticle remained stable for one week of storage without significant change of size and polydispersity index (PDI) as shown in Fig. 2

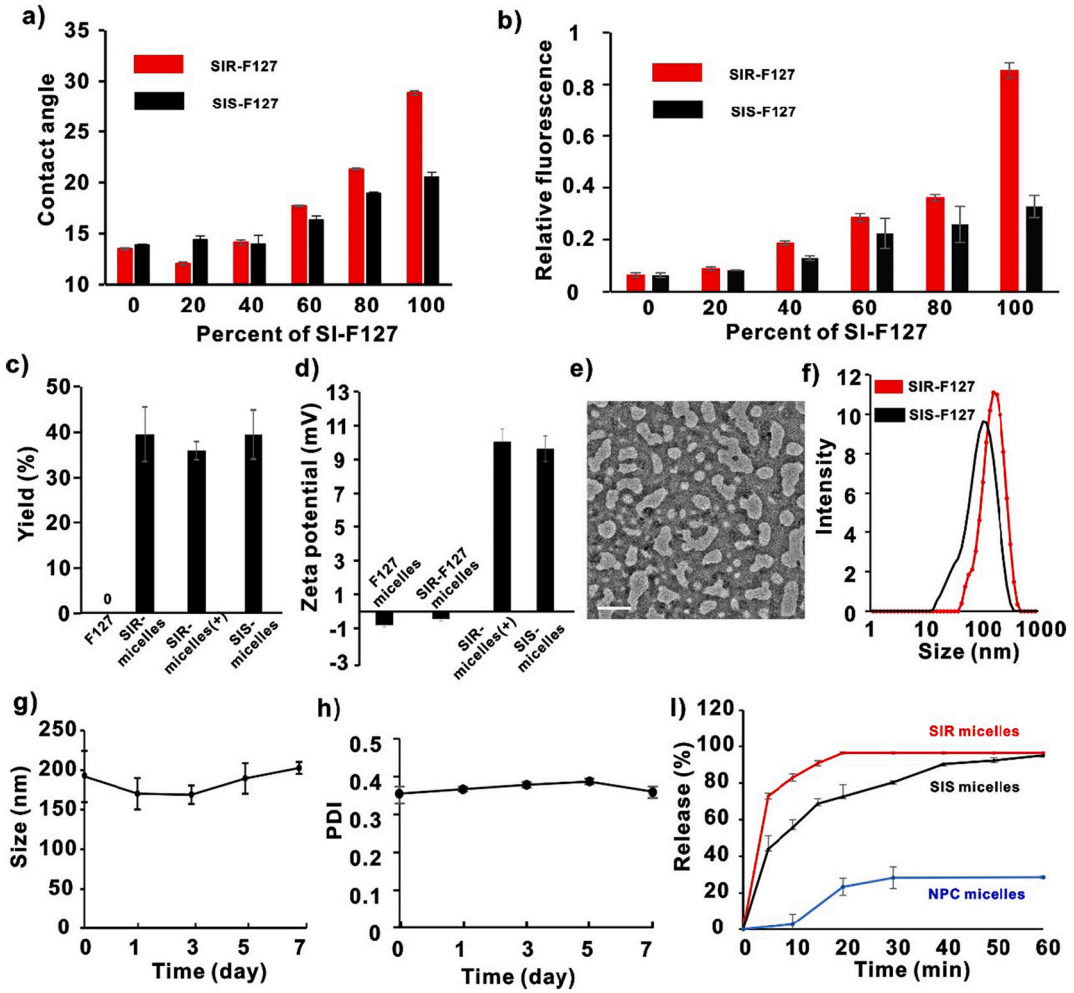

Fig. 2. Generation and characterization of SIR-micelles(+). a) Contact angle of 10 (wt)% blended polymers of F127 and SIR—F127. b) Cellular uptake of 10 (wt)% blended BPc-encapsulated micelles (blend of F127 and SIR-F127 or blend of F127 and SIS-F127) into macrophages. c) Encapsulation yield of colistin drug in 5 (wt)% F127, SIR-micelles and SIR-micelles(+), respectively. d) Zeta potential of regular F127 micelles, SIR-F127 micelles (without colistin crosslinking), and SIR-micelles (+) in aqueous solution. e) TEM images of SIR-micelles(+). Scale bar: 200 nm. f) Size distribution of SIR-micelles(+) measured by dynamic light scatting. g) Size stability and h) Polydispersity of SIR-micelles(+) during one week of storage at room temperature. i) Colistin release percent after SIR-micelles, SIS-micelles, NPC-micelles were reduced by 10 mM glutathione in dialysis bag.

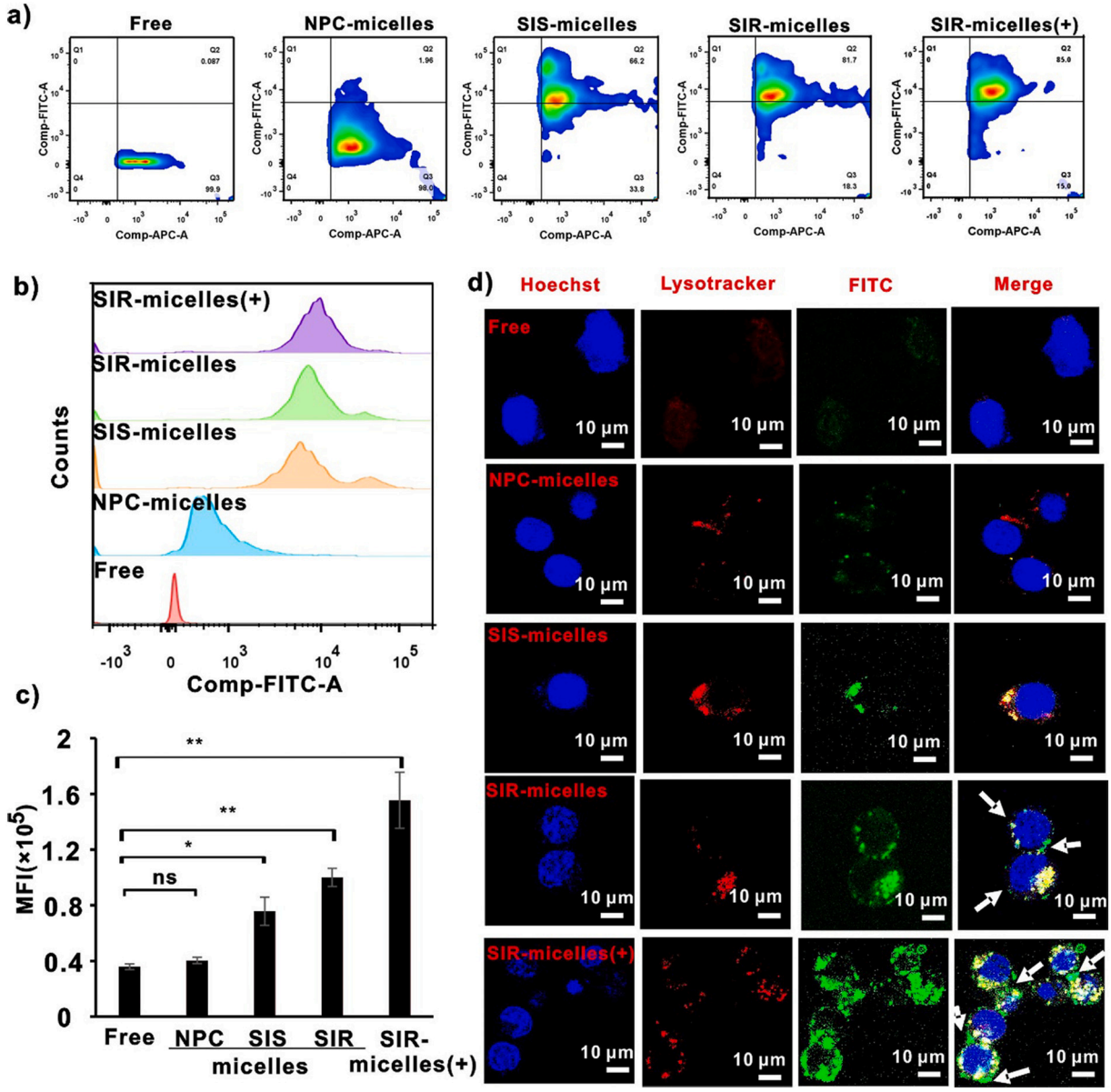

Fig. 3. Intracellular uptake *in vitro* of SIR-micelles. a) Distributions of different FITC-labeled colistin formations and APC-F4/80 antibody labeled macrophages in flow cytometry assay after co-culture for 4 h. b) The internalization of different colistin formations into J774A.1 macrophages characterized by FITC channel in flow cytometry. c) The mean intracellular fluorescence intensity of different formulations of FITC-labeled colistin after incubation with macrophages, followed by removal of extracellular colistin and lysis of macrophages. d) Laser scan confocal microscopic images of macrophages after incubation with different colistin formulations. Cell nucleus was stained with Hochest (blue); lysosomes was labeled with lysotracker (red); colistin drug was labeled with FITC (green). One-way analysis of variance (ANOVA) was used for significant difference analysis, $^{*}P < 0.05$, $^{**}P < 0.01$, $^{***}P < 0.001$. (For interpretation of the references to colour in this figure legend, the reader is referred to the web version of this article.)

g and h. SIR-micelles(+) were stable during incubation for 4 h in phosphate buffer solution (PBS) with 10 (wt)% FBS (fetal bovine serum), and remained 80% within 24 h because of less reducing agents existing in serum compared to intracellular environment with 2–3 orders of magnitude higher concentration of glutathione [38–40] (Fig. S9), which ensures the colistin not to pre-maturely release when circulating in blood. As shown in Fig. 2i, owing to the self-immolation moiety, upon reduction by glutathione, SIR-micelles and SIS-micelles released 100% of the colistin within 20 min and 60 min, respectively whereas NPC-micelles could only release less than 20% of the colistin within one hour and remained the same for at least 2 h.

3.3. *In vitro* uptake in macrophages

The cytotoxicity of colistin SIR-micelles(+) and free colistin to macrophages was first evaluated using CCK-8 viability test. As demonstrate in Fig. S10, 128 μg/mL of free colistin started to induce cytotoxicity whereas at least 256 μg/mL colistin SIR-micelles(+) (equivalent colistin concentration) did not induce noticeable toxicity in J774A.1 macrophages, a common type of intracellular bacteria host cell. This demonstrates that SIR-micelles(+) improved the safety profile compared to free colistin, and established that less than 256 μg/mL should be a safe dose for *in vitro* tests using macrophages. In the following *in vitro* experiments, 64 μg/mL SIR-micelles(+) was used.

Next, we evaluated the cellular uptake of various drug formations in J774A.1 macrophages by flow cytometry. Macrophages were incubated

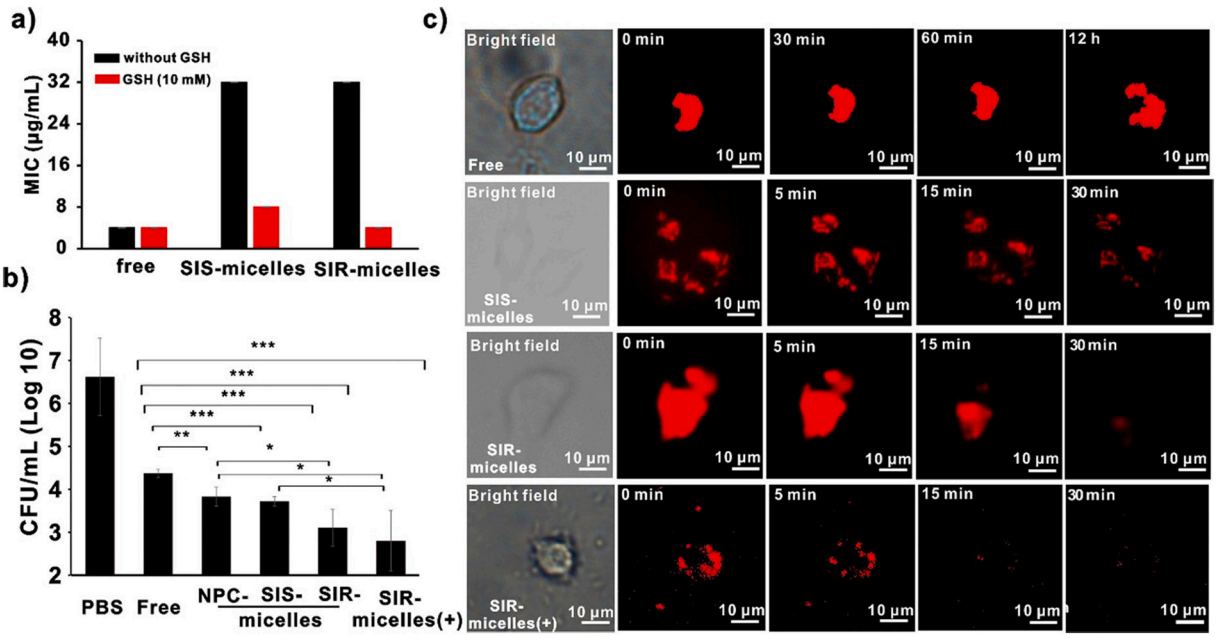

Fig. 4. Intracellular antimicrobial efficacy *in vitro* of SIR-micelles a) Minimum inhibitory concentrations (MICs) of various formations for *MDR-KP* with or with no addition of GSH. b) The CFUs of *MDR-KP* bacteria survived intracellularly after treatment with 64 μg/mL of various drug formations. c) Microscopic images of macrophages sequestering RFP (red fluorescence protein)-expressing *E. coli* after treatment by free colistin, SIS-micelles, SIR-micelles, and SIR-micelles(+). One-way analysis of variance (ANOVA) was used for significant difference analysis, $^{*}P < 0.05$, $^{**}P < 0.01$, $^{***}P < 0.001$. (For interpretation of the references to colour in this figure legend, the reader is referred to the web version of this article.)

with various FITC-labeled colistin formulations for 4 h, followed by labelling with anti-F4/80 antibody conjugated with allophycocyanine (APC) fluorophore (The gating strategy is based on F4/80 postive cells, Fig. S11). As shown in Fig. 3a-b, 81.7% of positive macrophages endocytosized colistin in SIR-micelles, compared to just 0.087% for the free colistin group and 1.96% of colistin for the NPC-micelle group. The addition of mannose improved the uptake ratio to 85.0% in the SIR-micelle(+) group owing to the targeting effect of mannose. Similarly, SIR-micelles(+) exhibited higher uptake in macrophages quantified by the FITC-labeling method after macrophages incubated with various colistin formulations were lysed by 1% Triton X-100 (Fig. 3c). Confocal microscopic images revealed that the signal of FITC-labeling colistin internalized into macrophages in various formulations followed the order of SIR-micelles(+) > SIR-micelles > SIS-micelles > NPC-micelles > free colistin as shown in Fig. S12, consistent with the results in Fig. 3b-c. Moreover, SIR-micelles and SIR-micelles(+) successfully escaped from lysosomes after the uptake by macrophages shown in Fig. 3d (indicated by white arrows), which may be attributed to the positive charge and hydrophobic moiety of SIR-micelles(+) [41]. The enhanced cellular uptake of SIR-micelles(+) compared to other formulations in macrophages could be explained by the factors below: (1) The bigger size of hydrophobically modified micelles (2) the hydrophobic moiety on the surface of micelles (3) the targeting ligand of mannose on SIR-micelles mediated the phagocytosis.

3.4. *In vitro* extracellular and intracellular antimicrobial activity

Next, we further investigated the antimicrobial effect of various formations on bacteria including *E. coli* MG 1655 and multidrug-resistant *Klebsiella pneumoniae* Y. 8401 (*MDR-KP*). We chose a clinically-relevant model of multidrug-resistant *K. pneumoniae* Y. 8401 (*MDR-KP*). The MICs against extracellular *MDR-KP* were measured in Fig. 4a. Because the amine groups of colistin were partially masked by SIS-micelles and SIR-micelles, they exhibited reduced antibacterial effects in the absence of GSH; In contrast, after cleavage of 10 mM GSH, SIR-micelles and SIS-micelles had almost the same antibacterial effect as the free colistin because the release of masked amines. Next, the intracellular antimicrobial efficacy of different colistin formulations including free colistin, NPC-micelles, SIS-micelles, SIR-micelles, and SIR-micelles(+) were studied using macrophages after incubation of each formulation and then removal of extracellular *MDR-KP*. As shown in Fig. 4b, the colony forming units (CFUs) in macrophages was significantly reduced by 1–2 orders of magnitude after the treatment by SIR-micelles or SIR-micelles(+), compared with free colistin and NPC-micelles. Besides, SIR-micelles performed slightly better intracellular antimicrobial activity than SIS-micelles *in vitro* with equivalent addition of colistin probably because of higher uptake by macrophages of SIR-micelles with stronger hydrophobicity and faster release rate within 20 min (Fig. 4b). Next, confocal microscopy was used to visualize and monitor the antimicrobial killing process. For generalization, another type of bacteria, RFP (red fluorescent protein)-expressing *E. coli* were incubated with macrophages for phagocytosis, followed by removal of extracellular bacteria using gentamycin. As shown in Fig. 4c, we chose various colistin formations for further comparison and found that using colistin SIR-micelles(+) for the treatment of intracellular *E. coli*, the red fluorescence signal was almost undetectable after only 15 min, indicating more rapid intracellular bacteria killing by SIR-micelles(+) than SIS-micelles due to more targeted uptake by macrophage and faster colistin release rate. Furthermore, the red fluorescence signal almost disappeared after incubation of SIR-micelles with intracellular *E. coli* for 30 min, which further revealed that targeted-mediated uptake enabled faster clearance of intracellular bacteria by SIR-micelles(+). In contrast, free colistin seems unable to kill intracellular *E. coli* after even at least 12 h, likely because it is difficult for small molecule of free colistin to be phagocytosed in cells. These results demonstrate that SIR-micelles(+) can be used as an effective antibiotic formulation to attenuate intracellular bacteria Additional microscopic images revealing the strong antimicrobial bactericidal efficacy of SIR-micelles(+) are shown in Fig. S13.

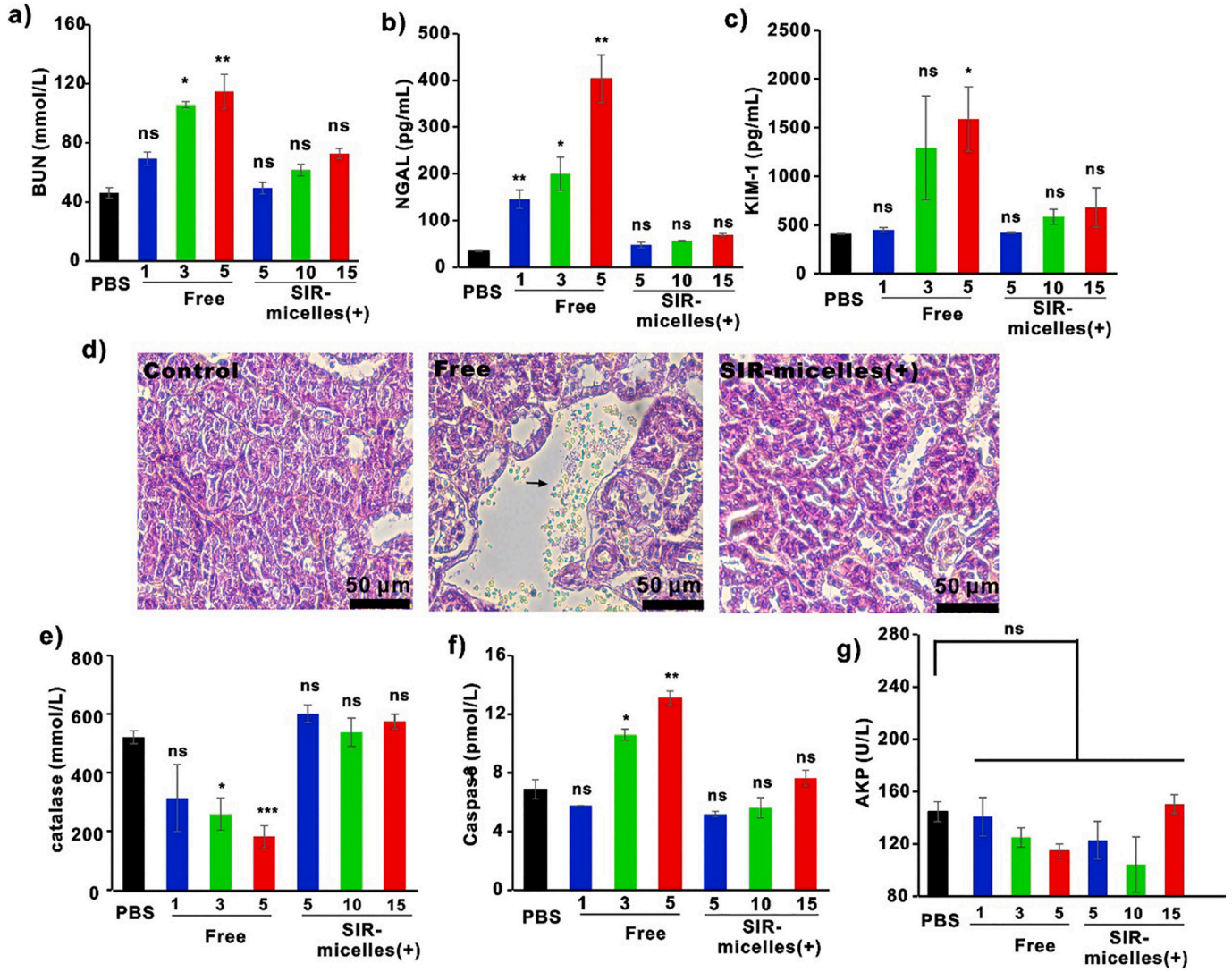

Fig. 5. Nephrotoxicity and neurotoxicity of mice induced by free colistin and SIR-micelles(+). Mice were given intravenously free colistin or SIR-micelles(+) of indicated doses daily for seven consecutive days, then the following biomarkers were measured. The levels of a) BUN and b) NGAL in serum 24 h after the last injection. c) The level of KIM-1 in urine 24 h after the last injection. d) Histopathological images kidney of mice given PBS, free colistin or SIR-micelles(+) after consecutive injections for seven days. e) Catalase and f) Caspase-3 in brain cerebrum 24 h after the last injection. g) AKP in serum 24 h after the last injection. $n = 3$ for PBS group; $n = 4$ for free colistin groups (1, 3, 5 mg/kg) and SIR-micelles(+) groups (5, 10, 15 mg/kg). One-way analysis of variance (ANOVA) was used for significant difference analysis, $^{*}P < 0.05$, $^{**}P < 0.01$, $^{***}P < 0.001$. The analysis of significant difference is compared with PBS group.

3.5. *In vivo evaluation of toxicity*

Given that nephrotoxicity and neurotoxicity are common side effects induced by colistin, we next investigated the toxicity of SIR-micelles(+) in comparison with free colistin. Outbred CD-1 mice were given 1, 3 or 5 mg/kg free colistin by intravenous tail injection every day for seven days. In contrast, we gave higher doses of SIR-micelles(+) (5, 10, 15 mg/kg) in the same treatment paradigm. The nephrotoxicity caused by polymyxin involves damage to the glomerulus filtration and the permeability of renal tubular cells [42]. We first measured the levels of blood urea nitrogen (BUN) and neutrophil gelatinase-associated lipocalin (NGAL), the commonly used biomarkers for the evaluation of renal damage [43]. As Fig. 5a demonstrates, mice treated with 3 mg/kg free colistin exhibited significantly increased level of BUN, whereas no significant increase was observed in SIR-micelle(+) group when given a dose of even 15 mg/kg. Similarly, the serum NGAL level, another more sensitive biomarker of nephrotoxicity, significantly increased compared to PBS group when mice were given only 1 mg/kg free colistin. For the mice given even 15 mg/kg colistin in SIR-micelles(+), no increase in NGAL levels were observed (Fig. 5b). We also assessed the level of kidney injury molecule-1 (KIM-1) in urine in Fig. 5c, showing that 5 mg/kg free colistin induced significant elevated level of KIM-1; In contrast, 5, 10, 15 mg/kg SIR-micelles did not give rise to significantly increased level of KIM-1 in serum compared with the PBS group. Renal injury was further confirmed by the histological structures of kidney in Fig. 5d. 5 mg/kg free colistin caused serious infiltration of inflammatory cells in the kidney tissue, whereas SIR-micelles(+) at the same dose did not induce pathological nephrotoxicity, similar as the control group given PBS. Taken together, these results show that the nephrotoxicity induced by free colistin could be reduced at least 5– 15 fold using the SIR-micelle (+) formulation.

Next, the neurotoxicity of colistin in SIR-micelles(+) or free colistin was assessed by measuring biomarkers of catalase and caspase-3, which reflect levels of oxidase stress and cell apoptosis in the central nervous tissue, respectively [44,45]. As shown in Fig. 5e-f, 3 mg/kg free colistin significantly reduced the catalase levels and elevated the caspase-3 levels in serum, indicative of oxidative stress and cell apoptosis in nerve tissues. However, the highest dose of 15 mg/kg colistin in SIR-

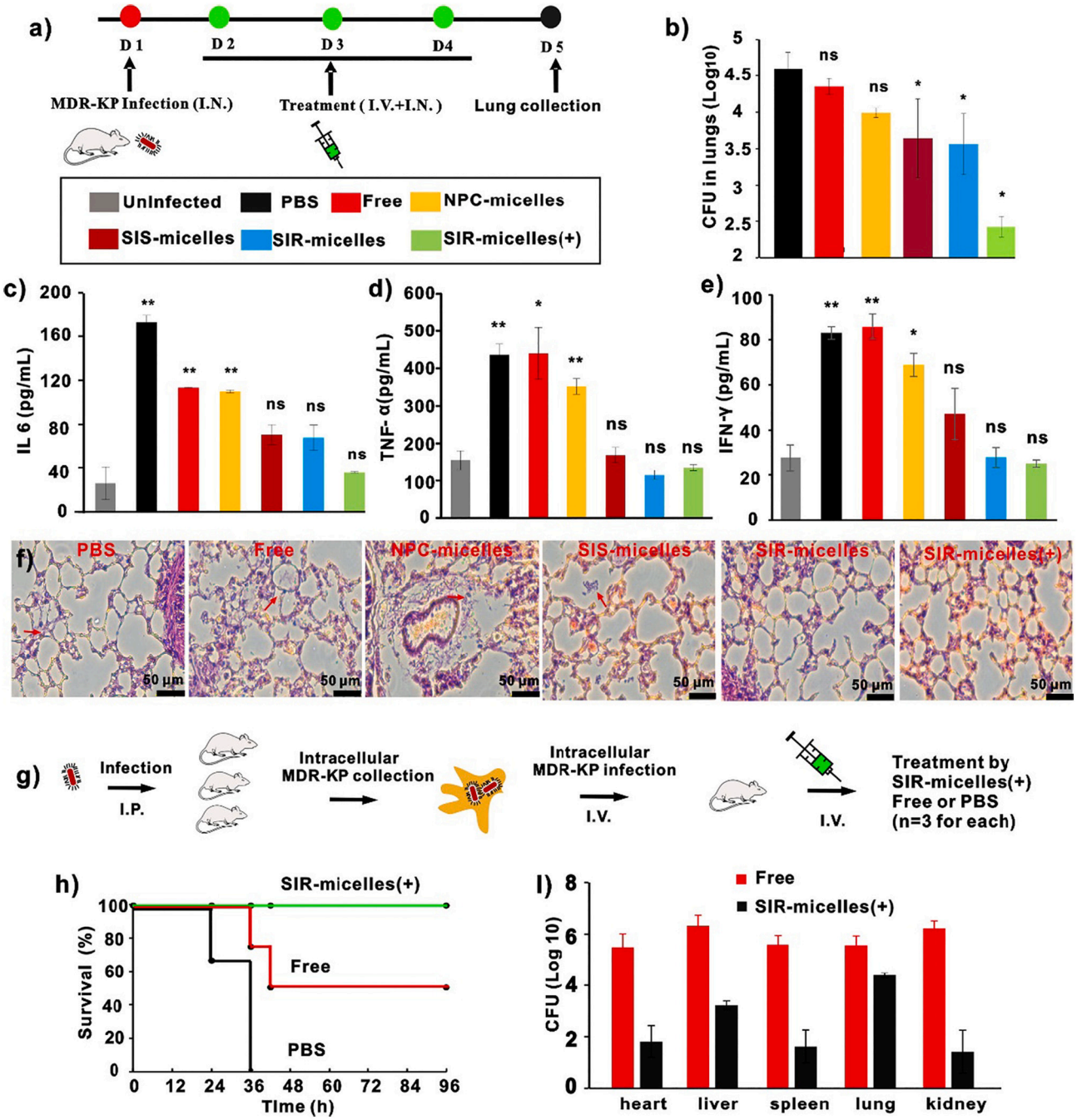

Fig. 6. *In vivo* treatment of pneumonia infection and transferred intracellular bacterial infection. a) Scheme of treatment for pneumonia infection using various colistin formulations ($n = 3$ for each group). b) CFUs of intracellular *MDR-KP* bacteria in lung tissue. The levels of c) IL-6, d) TNF-α, and e) IFN-γ in cells supernatant of lung tissue and bronchus after daily treatment by various colistin formulations for three days. f) Histopathological images of lung tissues in mice given colistin treatment. g) The schematic description of intracellular bacterial infection (n = 3 for each group). h) The survival rate of mice treated with PBS, free drug or SIR-micelles(+). i) The bacterial CFUs of organs of mice treated with free drug (red) and SIR-micelles(+) (black) for three consecutive days. $^{*}P < 0.05$, $^{**}P < 0.01$, $^{***}P < 0.001$. One-way analysis of variance (ANOVA) was used for significant difference analysis, The analysis of significant difference is compared with PBS group (a) and uninfected group (b-d). (For interpretation of the references to colour in this figure legend, the reader is referred to the web version of this article.)

micelles(+) did not induce change of catalase and caspase-3 in brain homogenates compared to mice given PBS. Weight loss of mice given free colistin was observed likely due to nephrotoxicity and neurotoxicity while the body weight of mice given 15 mg/kg colistin in SIR-micelles (+) increased by 10% (Fig. S14). Free colistin, as small molecules accumulate and get excreted in kidney whereas colistin SIR-micelles(+) were prone to accumulation in liver instead (Fig. 7). Therefore, we next also assessed the hepatotoxicity of SIR-micelles(+) with the control of PBS and free colistin. Mice were intravenously given PBS, 5 mg/kg colistin SIR-micelles(+), and 5 mg/kg free colistin daily for seven days. As shown in Fig. 5g, the levels of alkaline phosphatase (AKP) in PBS, free colistin and SIR-micelles(+) were almost the same with no significant difference.

3.6. SIR-micelles for pneumonia infection treatment in vivo

Encouraged by the antimicrobial efficacy and safety *in vitro*, we next assessed the therapeutic effect of SIR-micelles for treating intracellular

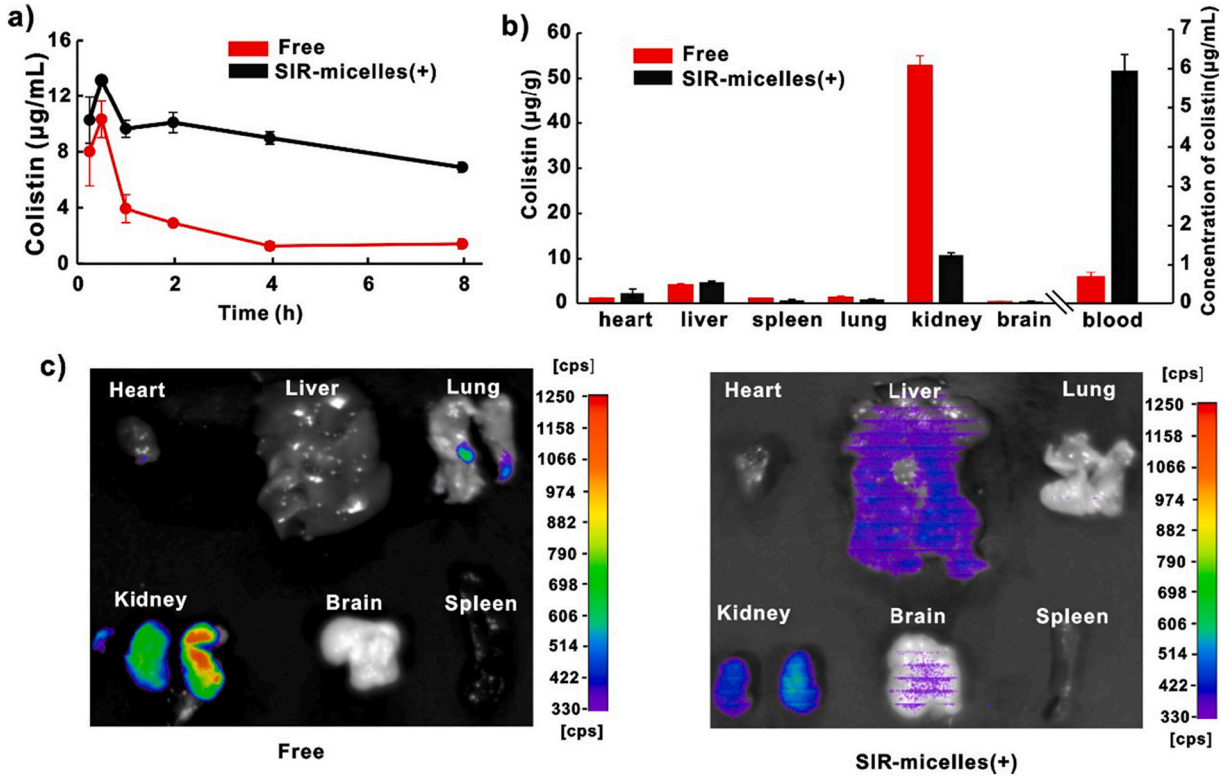

Fig. 7. The pharmacokinetics and biodistribution 24 h after intravenously injection of free drug (red) or SIR-micelles(+) (black). a) concentrations of drugs in plasma at different timepoints as indicated b) Concentration of colistin in organs and c) Fluorescence imaging of organs including heart, liver, spleen, lung, kidney and brain after mice were given FITC-labeled free drug (left) and SIR-micelles(+) (right) and sacrificed at 24 h ($n = 3$ for each group). (For interpretation of the references to colour in this figure legend, the reader is referred to the web version of this article.)

bacteria *in vivo*. A pneumonia infection model was established by intranasal administration of *MDR-KP* in mice on day 0, followed by both intravenous (5 mg/kg) and intranasal (1 mg/kg) injection of SIR-micelles daily for three consecutive days. On day 4, lung tissues were collected. Subsequently, extracellular bacteria were killed by gentamycin and CFUs of intracellular *MDR-KP* was counted after culturing for overnight (See Fig. 6a for the treatment scheme). As shown in Fig. 6b, free colistin and NPC-micelles did not significantly reduce the number of intracellular bacteria compared to PBS group whereas both colistin SIR-micelles and SIS-micelles significantly alleviated the intracellular bacterial burden by about an order of magnitude. Particularly, with the conjugation of mannose ligand, colistin SIR-micelles(+) reduced the CFUs in lung cells by about two orders of magnitude (Fig. 6b). We also measured the levels of inflammatory cytokines (IL-6, TNF-α, IFN-γ) in the extract supernatant of lung tissue cells to further evaluate the damage of bacterial infection to lung tissues since these cytokines are usually used as sensitive markers of inflammation caused by infections, immune homeostasis, trauma or injures [46]. As shown in Fig. 6c-e, the levels of the three cytokines in mice were significantly raised when mice were treated with PBS, free colistin or NPC-micelles compared to healthy mice left uninfected and untreated. By contrast, the concentrations of IL-6, TNF-α or IFN-γ did not significantly change when mice were given SIS-micelles, SIR-micelles or SIR-micelles(+). These results could possibly be explained by the fact that hydrophobic modification of F127 micelles using self-immolative linkers facilitated the cellular uptake and traceless release of pristine colistin. It appears that the antimicrobial *in vitro* and *in vivo* efficacy of the SIR-micelles is only slightly better than SIS-micelles without significant differece, which could be explained by the fact that both micelles can release all colistin in 12 h or 24 h. However, as shown in Fig. 2I and 4C, SIR-micelles could release 100% colistin within 20 min but SIS-micelle needs 1 h to fully release colistin. This improvement could be clinically important for the management of the acute diseases that require urgent care. Given the exponential growth rate of bacteria, antibiotic therapy needs sufficient concentration of drugs that should be released in a timely manner at the infection sites [47,48]. We also examined the histological images of the lung tissues from each group. As shown in Fig. 6f, the infiltration of inflammatory cells in lung tissues, indicated by arrows, was observed in the groups of PBS, free, NPC-micelles, SIS-micelles, similarly as the previously published results [49]. By contrast, mice treated with SIR-micelles or SIR-micelles(+) showed no noticeable inflammatory infiltration in lung cells. These results indicated that SIR-micelles(+) can be effectively used for the treatment of intracellular bacterial infection. Also, intravenous administration alone of SI-micelles could effectively relieve the bacterial burden of pneumonia tissues and corresponding inflammatory cytokines as well (Fig. S15), although the targeting effect of mannose was not as pronounced as the combination of intravenous and intranasal treatment.

We also found that higher virulence seemed to be induced when mice were infected by *MDR-KP* sequestered inside macrophages or neutrophils extracted from donor mice infected beforehand because the mice had the symptoms of slow movement and piloerection, which were not observed in those infected with *MDR-KP* taken directly from broth culture (Fig. 6a and g). It has been also reported that infection by intracellular bacteria led to higher bacterial burden in tissues than those infected with planktonic bacteria [50]. Therefore, we next assessed the use of SIR-micelles for the treatment of such more serious infection scenario. Intracellular bacterial infection was established by intravenous injection of the cells extracted from donor mice that beforehand received *MDR-KP* infection *via* intraperitoneally into acceptor mice. Then acceptor mice were treated with 5 mg/kg free drug or SIR-micelles intravenously daily for three consecutive days. As shown in Fig. 6h, all mice treated with PBS died within 36 h whereas 50% mice died within 96 h if given free colistin [51]. After treatment by SIR-micelles(+), the

survival rate of mice remained 100%. Then, organs of heart, liver, spleen, lung, kidney were collected and the CFUs of bacteria in homogenates of organs were measured. As demonstrated in Fig. 6i, SIR-micelles(+) alleviated the bacterial burden in organs by about 4– 5 orders of magnitude compared with free group (except lung tissue where the CFUs of bacteria were reduced by about 100 times). In order to shed light on the good antimicrobial effect and reduced toxicity of SIR-micelles, we further investigated their pharmacokinetics and biodistribution properties [52]. As shown in Fig. 7a, SIR-micelles(+) extended the half-life of colistin in plasma up to about 8 h, which was about 16 times higher than that in free colistin. The biodistribution of colistin in organs in Fig. 7b-c revealed that free colistin was prone to accumulate in kidneys, while SIR-micelles(+) significantly reduced the accumulation of drug in kidneys. Although more colistin SIR-micelles (+) accumulated in liver compared to free colistin, no significant hepatotoxicity was observed shown in Fig. 5g.

4. Conclusion

We designed two reduction-responsive self-immolative linkers that can facilitate the intracellular uptake and traceless release pristine colistin. Next, we introduced the antibiotic-crosslinking strategy to generate self-immolative SIR-micelles(+) that can load hydrophilic colistin with good stability. Hydrophobic modification enabled enhanced phagocytosis of SIR-micelles(+) in macrophage where intracellular bacteria colonize. Mannose can be easily conjugated on the SIR-micelles in aqueous solution, enabling targeting delivery of colistin to macrophages. Intracellular glutathione cleave SIR-micelles(+) rapidly, releasing pristine colistin that can effectively treat intracellular infections in lungs and a transferred intracellular infection model. Taken together, SIR-micelle(+), as a new antimicrobial biomaterials warrants further investigation for the treatment of intracellular infections.

Author contributions

Xingyue Yang and Yumiao Zhang conceived and designed the project. Xingyue Yang carried out most experiments. Qian Qiu assisted with cell experiments and animal experiments. Gengqi Liu assisted with material synthesis. He Ren and Xiaojie Wang assisted with animal experiments. Xingyue Yang, Yumiao Zhang, and Jonathan F. Lovell wrote the manuscript.

Declaration of Competing Interest

The authors declare that they have no known competing financial interests or personal relationships that could have appeared to influence the work reported in this paper.

Acknowledgments

This work was supported by the National Key Research and Development Program (2021YFC2102300), National Natural Science Foundation of China (32071384), Start-up Grant at Tianjin University and One-thousand Young Talent Program of China. We thank Prof. Pengfei Wang at Shanghai Jiao Tong University for kindly providing the bacteria of *MDR-KP*.

Appendix A. Supplementary data

Supplementary data to this article can be found online at https://doi.org/10.1016/j.jconrel.2021.11.037.

References

[1] S. Helaine, A.M. Cheverton, K.G. Watson, L.M. Faure, S.A. Matthews, D.W. Holden, Internalization of Salmonella by macrophages induces formation of nonreplicating persisters, Science. 343 (2014) 204–208, https://doi.org/10.1126/science.1244705.
[2] G.E. Thwaites, V. Gant, Are bloodstream leukocytes Trojan horses for the metastasis of Staphylococcus aureus? Nat. Rev. Microbiol. 9 (2011) 215–222, https://doi.org/10.1038/nrmicro2508.
[3] K. Ray, B. Marteyn, P.J. Sansonetti, C.M. Tang, Life on the inside: the intracellular lifestyle of cytosolic bacteria, Nat. Rev. Microbiol. 7 (2009) 333–340, https://doi.org/10.1038/nrmicro2112.
[4] G. Mitchell, C. Chen, D.A. Portnoy, Strategies used by bacteria to grow in macrophages, Microbiol. Spectr. 4 (2016), https://doi.org/10.1128/microbiolspec.MCHD-0012-2015.
[5] H. Sahly, R. Podschun, Clinical, bacteriological, and serological aspects of Klebsiella infections and their spondylarthropathic sequelae, Clin. Diagn. Lab. Immunol. 4 (1997) 393–399, https://doi.org/10.1128/cdli.4.4.393-399.1997.
[6] Z.-Q. Yang, Y.-L. Huang, H.-W. Zhou, R. Zhang, K. Zhu, Persistent carbapenem-resistant Klebsiella pneumoniae: a Trojan horse, Lancet Infect. Dis. 18 (2018) 22–23, https://doi.org/10.1016/S1473-3099(17)30627-8.
[7] V. Cano, C. March, J.L. Insua, N. Aguiló, E. Llobet, D. Moranta, V. Regueiro, G. P. Brennan, M.I. Millán-Lou, C. Martín, J. Garmendia, J.A. Bengoechea, Klebsiella pneumoniae survives within macrophages by avoiding delivery to lysosomes, Cell. Microbiol. 17 (2015) 1537–1560, https://doi.org/10.1111/cmi.12466.
[8] Y. Pei, Y. Yeo, Drug delivery to macrophages: challenges and opportunities, J. Control. Release 240 (2016) 202–211, https://doi.org/10.1016/j.jconrel.2015.12.014.
[9] I.A. Bakker-Woudenberg, M.T. ten Kate, L.E. Stearne-Cullen, M.C. Woodle, Efficacy of gentamicin or ceftazidime entrapped in liposomes with prolonged blood circulation and enhanced localization in Klebsiella pneumoniae-infected lung tissue, J. Infect. Dis. 171 (1995) 938–947, https://doi.org/10.1093/infdis/171.4.938.
[10] Y.-C. Huang, R.-Y. Li, J.-Y. Chen, J.-K. Chen, Biphasic release of gentamicin from chitosan/fucoidan nanoparticles for pulmonary delivery, Carbohydr. Polym. 138 (2016) 114–122, https://doi.org/10.1016/j.carbpol.2015.11.072.
[11] L. Jiang, M.K. Greene, J.L. Insua, J.S. Pessoa, D.M. Small, P. Smyth, A.P. McCann, F. Cogo, J.A. Bengoechea, C.C. Taggart, C.J. Scott, Clearance of intracellular Klebsiella pneumoniae infection using gentamicin-loaded nanoparticles, J. Control. Release 279 (2018) 316–325, https://doi.org/10.1016/j.jconrel.2018.04.040.
[12] T.A. Dietsche, H.E. Eldesouky, S.M. Zeiders, M.N. Seleem, J. Chmielewski, Targeting intracellular pathogenic Bacteria through N-terminal modification of cationic amphiphilic Polyproline helices, J. Organomet. Chem. 85 (2020) 7468–7475, https://doi.org/10.1021/acs.joc.0c00871.
[13] F.-Y. Su, S. Srinivasan, B. Lee, J. Chen, A.J. Convertine, T.E. West, D.M. Ratner, S. J. Skerrett, P.S. Stayton, Macrophage-targeted drugamers with enzyme-cleavable linkers deliver high intracellular drug dosing and sustained drug pharmacokinetics against alveolar pulmonary infections, J. Control. Release 287 (2018) 1–11, https://doi.org/10.1016/j.jconrel.2018.08.014.
[14] S. Xie, S. Li, Z. Zhang, M. Chen, P. Ran, X. Li, Bacterial ghosts for targeting delivery and subsequent responsive release of ciprofloxacin to destruct intracellular bacteria, Chem. Eng. J. 399 (2020), 125700, https://doi.org/10.1016/j.cej.2020.125700.
[15] H. Zazo, C.I. Colino, J.M. Lanao, Current applications of nanoparticles in infectious diseases, J. Control. Release 224 (2016) 86–102, https://doi.org/10.1016/j.jconrel.2016.01.008.
[16] M.G. Elnaggar, K. Jiang, H.E. Eldesouky, Y. Pei, J. Park, S.A. Yuk, F. Meng, A. M. Dieterly, H.T. Mohammad, Y.A. Hegazy, H.M. Tawfeek, A.A. Abdel-Rahman, A. E. Aboutaleb, M.N. Seleem, Y. Yeo, Antibacterial nanotruffles for treatment of intracellular bacterial infection, Biomaterials. 262 (2020), 120344, https://doi.org/10.1016/j.biomaterials.2020.120344.
[17] S. Yang, X. Han, Y. Yang, H. Qiao, Z. Yu, Y. Liu, J. Wang, T. Tang, Bacteria-targeting nanoparticles with microenvironment-responsive antibiotic release to eliminate intracellular Staphylococcus aureus and associated infection, ACS Appl. Mater. Interfaces 10 (2018) 14299–14311, https://doi.org/10.1021/acsami.7b15678.
[18] X. Hou, X. Zhang, W. Zhao, C. Zeng, B. Deng, D.W. McComb, S. Du, C. Zhang, W. Li, Y. Dong, Vitamin lipid nanoparticles enable adoptive macrophage transfer for the treatment of multidrug-resistant bacterial sepsis, Nat. Nanotechnol. 15 (2020) 41–46, https://doi.org/10.1038/s41565-019-0600-1.
[19] Y. Liu, Y. Ren, Y. Li, L. Su, Y. Zhang, F. Huang, J. Liu, J. Liu, T.G. van Kooten, Y. An, L. Shi, H.C. van der Mei, H.J. Busscher, Nanocarriers with conjugated antimicrobials to eradicate pathogenic biofilms evaluated in murine in vivo and human ex vivo infection models, Acta Biomater. 79 (2018) 331–343, https://doi.org/10.1016/j.actbio.2018.08.038.
[20] M. Chen, J. He, S. Xie, T. Wang, P. Ran, Z. Zhang, X. Li, Intracellular bacteria destruction via traceable enzymes-responsive release and deferoxamine-mediated ingestion of antibiotics, J. Control. Release 322 (2020) 326–336, https://doi.org/10.1016/j.jconrel.2020.03.037.
[21] M.E. Falagas, S.K. Kasiakou, Colistin: the revival of polymyxins for the management of multidrug-resistant gram-negative bacterial infections, Clin. Infect. Dis. 40 (2005) 1333–1341, https://doi.org/10.1086/429323.
[22] E. Ozyilmaz, F.A. Ebinc, U. Derici, O. Gulbahar, G. Goktas, C. Elmas, I. K. Oguzulgen, S. Sindel, Could nephrotoxicity due to colistin be ameliorated with the use of N-acetylcysteine? Intensive Care Med. 37 (2011) 141–146, https://doi.org/10.1007/s00134-010-2038-7.
[23] D.J. Price, D.I. Graham, Effects of large doses of colistin sulphomethate sodium on renal function, Br. Med. J. 4 (1970) 525–527, https://doi.org/10.1136/bmj.4.5734.525.

[24] C. Dai, G.D. Ciccotosto, R. Cappai, Y. Wang, S. Tang, D. Hoyer, E.K. Schneider, T. Velkov, X. Xiao, Rapamycin confers neuroprotection against colistin-induced oxidative stress, mitochondria dysfunction, and apoptosis through the activation of autophagy and mTOR/Akt/CREB signaling pathways, ACS Chem. Neurosci. 9 (2018) 824–837, https://doi.org/10.1021/acschemneuro.7b00323.
[25] X. Yang, H. Ren, H. Zhang, G. Liu, Z. Jiang, Q. Qiu, C. Yu, N. Murthy, K. Zhao, J. F. Lovell, Y. Zhang, Antibiotic cross-linked micelles with reduced toxicity for multidrug-resistant bacterial Sepsis treatment, ACS Appl. Mater. Interfaces 13 (2021) 9630–9642, https://doi.org/10.1021/acsami.0c21459.
[26] S.L. Nielsen, F.T. Black, Extracellular and intracellular killing in neutrophil granulocytes of Staphylococcus aureus with rifampicin in combination with dicloxacillin or fusidic acid, J. Antimicrob. Chemother. 43 (1999) 407–410, https://doi.org/10.1093/jac/43.3.407.
[27] J. Turnidge, M.L. Grayson, Optimum treatment of staphylococcal infections, Drugs. 45 (1993) 353–366, https://doi.org/10.2165/00003495-199345030-00004.
[28] E.H. Lee, S.Y. Baek, J.Y. Park, Y.W. Kim, Rifampicin activates AMPK and alleviates oxidative stress in the liver as mediated with Nrf2 signaling, Chem. Biol. Interact. 315 (2020), 108889, https://doi.org/10.1016/j.cbi.2019.108889.
[29] A. Forsgren, A. Bellahsène, Antibiotic accumulation in human polymorphonuclear leucocytes and lymphocytes, Scand. J. Infect. Dis. Suppl. 44 (1985) 16–23.
[30] Y. Zhang, M. Jeon, L.J. Rich, H. Hong, J. Geng, Y. Zhang, S. Shi, T.E. Barnhart, P. Alexandridis, J.D. Huizinga, M. Seshadri, W. Cai, C. Kim, J.F. Lovell, Non-invasive multimodal functional imaging of the intestine with frozen micellar naphthalocyanines, Nat. Nanotech. 9 (2014) 631–638, https://doi.org/10.1038/nnano.2014.130.
[31] Y. Zhang, D. Wang, S. Goel, B. Sun, U. Chitgupi, J. Geng, H. Sun, T.E. Barnhart, W. Cai, J. Xia, J.F. Lovell, Surfactant-stripped frozen Pheophytin micelles for multimodal gut imaging, Adv. Mater. 28 (2016) 8524–8530, https://doi.org/10.1002/adma.201602373.
[32] Y. Zhang, W. Song, J. Geng, U. Chitgupi, H. Unsal, J. Federizon, J. Rzayev, D. K. Sukumaran, P. Alexandridis, J.F. Lovell, Therapeutic surfactant-stripped frozen micelles, Nat. Commun. 7 (2016) 11649, https://doi.org/10.1038/ncomms11649.
[33] Z. Jiang, B. Sun, Y. Wang, H. Gao, H. Ren, H. Zhang, T. Lu, X. Ren, W. Wei, X. Wang, L. Zhang, J. Li, D. Ding, J.F. Lovell, Y. Zhang, Surfactant-stripped micelles with aggregation-induced enhanced emission for bimodal gut imaging in vivo and microbiota tagging ex vivo, Adv. Healthc. Mater. (2021) 2100356, https://doi.org/10.1002/adhm.202100356, n/a.
[34] M.D. Resh, Trafficking and signaling by fatty-acylated and prenylated proteins, Nat. Chem. Biol. 2 (2006) 584–590, https://doi.org/10.1038/nchembio834.
[35] D. Missirlis, H. Khant, M. Tirrell, Mechanisms of peptide amphiphile internalization by SJSA-1 cells in vitro, Biochemistry. 48 (2009) 3304–3314, https://doi.org/10.1021/bi802356k.
[36] M. Wang, K. Alberti, S. Sun, C.L. Arellano, Q. Xu, Combinatorially designed lipid-like nanoparticles for intracellular delivery of cytotoxic protein for cancer therapy, Angew. Chem. Int. Ed. Eng. 53 (2014) 2893–2898, https://doi.org/10.1002/anie.201311245.
[37] G. Liu, J.F. Lovell, L. Zhang, Y. Zhang, Stimulus-responsive nanomedicines for disease diagnosis and treatment, Int. J. Mol. Sci. 21 (2020) 6380, https://doi.org/10.3390/ijms21176380.
[38] G. Liu, Z. Jiang, J.F. Lovell, L. Zhang, Y. Zhang, Design of a Thiol-Responsive, traceless prodrug with rapid self-immolation for Cancer chemotherapy, ACS Appl. Bio Mater. 4 (2021) 4982–4989, https://doi.org/10.1021/acsabm.1c00247.
[39] G. Wu, Y.-Z. Fang, S. Yang, J.R. Lupton, N.D. Turner, Glutathione metabolism and its implications for health, J. Nutr. 134 (2004) 489–492, https://doi.org/10.1093/jn/134.3.489.
[40] S.P. Hadipour Moghaddam, M. Yazdimamaghani, H. Ghandehari, Glutathione-sensitive hollow mesoporous silica nanoparticles for controlled drug delivery, J. Control. Release 282 (2018) 62–75, https://doi.org/10.1016/j.jconrel.2018.04.032.
[41] Z. Zha, J. Li, Z. Ge, Endosomal-escape polymers based on multicomponent reaction-synthesized monomers integrating alkyl and Imidazolyl moieties for efficient gene delivery, ACS Macro Lett. 4 (2015) 1123–1127, https://doi.org/10.1021/acsmacrolett.5b00615.
[42] C. Dai, S. Tang, S. Deng, S. Zhang, Y. Zhou, T. Velkov, J. Li, X. Xiao, Lycopene attenuates colistin-induced nephrotoxicity in mice via activation of the Nrf2/HO-1 pathway, Antimicrob. Agents Chemother. 59 (2015) 579–585, https://doi.org/10.1128/AAC.03925-14.
[43] J. Huang, J. Li, Y. Lyu, Q. Miao, K. Pu, Molecular optical imaging probes for early diagnosis of drug-induced acute kidney injury, Nat. Mater. 18 (2019) 1133–1143, https://doi.org/10.1038/s41563-019-0378-4.
[44] C. Dai, X. Xiao, J. Li, G.D. Ciccotosto, R. Cappai, S. Tang, E.K. Schneider-Futschik, D. Hoyer, T. Velkov, J. Shen, Molecular mechanisms of neurotoxicity induced by Polymyxins and chemoprevention, ACS Chem. Neurosci. 10 (2019) 120–131, https://doi.org/10.1021/acschemneuro.8b00300.
[45] M.Y. Kang, H.-B. Kim, C. Piao, K.H. Lee, J.W. Hyun, I.-Y. Chang, H.J. You, The critical role of catalase in prooxidant and antioxidant function of p53, Cell Death Differ. 20 (2013) 117–129, https://doi.org/10.1038/cdd.2012.102.
[46] S.A. Jones, B.J. Jenkins, Recent insights into targeting the IL-6 cytokine family in inflammatory diseases and cancer, Nat. Rev. Immunol. 18 (2018) 773–789, https://doi.org/10.1038/s41577-018-0066-7.
[47] M.E. Falagas, S.K. Kasiakou, S. Tsiodras, A. Michalopoulos, The use of intravenous and aerosolized Polymyxins for the treatment of infections in critically ill patients: a review of the recent literature, Clin. Med. Res. 4 (2006) 138–146, https://doi.org/10.3121/cmr.4.2.138.
[48] A.A. Udy, J.A. Roberts, J. Lipman, Clinical implications of antibiotic pharmacokinetic principles in the critically ill, Intensive Care Med. 39 (2013) 2070–2082, https://doi.org/10.1007/s00134-013-3088-4.
[49] A.O. Hassan, J.B. Case, E.S. Winkler, L.B. Thackray, N.M. Kafai, A.L. Bailey, B. T. McCune, J.M. Fox, R.E. Chen, W.B. Alsoussi, J.S. Turner, A.J. Schmitz, T. Lei, S. Shrihari, S.P. Keeler, D.H. Fremont, S. Greco, P.B. McCray, S. Perlman, M. J. Holtzman, A.H. Ellebedy, M.S. Diamond, A SARS-CoV-2 infection model in mice demonstrates protection by neutralizing antibodies, Cell. 182 (2020) 744–753.e4, https://doi.org/10.1016/j.cell.2020.06.011.
[50] S.M. Lehar, T. Pillow, M. Xu, L. Staben, K.K. Kajihara, R. Vandlen, L. DePalatis, H. Raab, W.L. Hazenbos, J.H. Morisaki, J. Kim, S. Park, M. Darwish, B.-C. Lee, H. Hernandez, K.M. Loyet, P. Lupardus, R. Fong, D. Yan, C. Chalouni, E. Luis, Y. Khalfin, E. Plise, J. Cheong, J.P. Lyssikatos, M. Strandh, K. Koefoed, P. S. Andersen, J.A. Flygare, M. Wah Tan, E.J. Brown, S. Mariathasan, Novel antibody-antibiotic conjugate eliminates intracellular S. aureus, Nature. 527 (2015) 323–328, https://doi.org/10.1038/nature16057.
[51] H.J. Busscher, W. Woudstra, T.G. van Kooten, P. Jutte, L. Shi, J. Liu, W.L. J. Hinrichs, H.W. Frijlink, R. Shi, J. Liu, J. Parvizi, S. Kates, V.M. Rotello, T. P. Schaer, D. Williams, D.W. Grainger, H.C. van der Mei, Accepting higher morbidity in exchange for sacrificing fewer animals in studies developing novel infection-control strategies, Biomaterials. 232 (2020), 119737, https://doi.org/10.1016/j.biomaterials.2019.119737.
[52] P. Cheng, K. Pu, Molecular imaging and disease theranostics with renal-clearable optical agents, Nat. Rev. Mater. (2021) 1–19, https://doi.org/10.1038/s41578-021-00328-6.